



# Early events of fertilization in sea urchin eggs are sensitive to actin-binding organic molecules

Jong T. Chun <sup>\*</sup>, Nunzia Limatola, Filip Vasilev, Luigia Santella

Stazione Zoologica Anton Dohrn, Villa Comunale 1, Napoli I-80121, Italy



## ARTICLE INFO

### Article history:

Received 30 May 2014

Available online 21 June 2014

### Keywords:

Cortical flash

Polyspermy

Actin

Cortical granules exocytosis

Calcium signaling

## ABSTRACT

We previously demonstrated that many aspects of the intracellular  $\text{Ca}^{2+}$  increase in fertilized eggs of starfish are significantly influenced by the state of the actin cytoskeleton. In addition, the actin cytoskeleton appeared to play comprehensive roles in modulating cortical granules exocytosis and sperm entry during the early phase of fertilization. In the present communication, we have extended our work to sea urchin which is believed to have bifurcated from the common ancestor in the phylogenetic tree some 500 million years ago. To corroborate our earlier findings in starfish, we have tested how the early events of fertilization in sea urchin eggs are influenced by four different actin-binding drugs that promote either depolymerization or stabilization of actin filaments. We found that all the actin drugs commonly blocked sperm entry in high doses and significantly reduced the speed of the  $\text{Ca}^{2+}$  wave. At low doses, however, cytochalasin B and phalloidin increased the rate of polyspermy. Overall, certain aspects of  $\text{Ca}^{2+}$  signaling in these eggs were in line with the morphological changes induced by the actin drugs. That is, the time interval between the cortical flash and the first  $\text{Ca}^{2+}$  spot at the sperm interaction site (the latent period) was significantly prolonged in the eggs pretreated with cytochalasin B or latrunculin A, whereas the  $\text{Ca}^{2+}$  decay kinetics after the peak was specifically attenuated in the eggs pretreated with jasplakinolide or phalloidin. In addition, the sperm interacting with the eggs pretreated with actin drugs often generated multiple  $\text{Ca}^{2+}$  waves, but tended to fail to enter the egg. Thus, our results indicated that generation of massive  $\text{Ca}^{2+}$  waves is neither indicative of sperm entry nor sufficient for cortical granules exocytosis in the inseminated sea urchin eggs, whereas the structure and functionality of the actin cytoskeleton are the major determining factors in the two processes.

© 2014 Elsevier Inc. All rights reserved.

## 1. Introduction

One of the first changes taking place in the fertilized eggs of nearly all animal species is an increase of intracellular  $\text{Ca}^{2+}$ , which is utilized as a second messenger to initiate a cascade of subsequent egg activation procedures [1–3]. In fertilized sea urchin eggs, the intracellular  $\text{Ca}^{2+}$  increase has two components: the rapid synchronized influx of external  $\text{Ca}^{2+}$  via L-type  $\text{Ca}^{2+}$  channels and the subsequent global  $\text{Ca}^{2+}$  wave that propagates from the sperm interaction site to the antipode [4–8]. A similar pattern of  $\text{Ca}^{2+}$  signaling has also been observed in fertilized eggs of starfish, and the intracellular  $\text{Ca}^{2+}$  increases in echinoderm eggs have been

**Abbreviations:** PIP2, phosphatidylinositol-4,5-bisphosphate;  $\text{InsP}_3$ , inositol trisphosphate; cADPr, cyclic ADP ribose; NAADP, nicotinic acid adenine dinucleotide phosphate; RFU, relative fluorescence unit; CYT-B, cytochalasin B; LAT-A, latrunculin A; JAS, jasplakinolide; PHAL, phalloidin; FE, fertilization envelope.

<sup>\*</sup> Corresponding author. Fax: +39 081 764 1355.

E-mail address: [chun@szn.it](mailto:chun@szn.it) (J.T. Chun).

<http://dx.doi.org/10.1016/j.bbrc.2014.06.057>

0006-291X/© 2014 Elsevier Inc. All rights reserved.

recapitulated in large part by the second messengers that induce  $\text{Ca}^{2+}$  release from the internal stores, e.g.  $\text{InsP}_3$ , cADPr, and NAADP [9–11].

During the course of our studies on the molecular mechanisms of  $\text{Ca}^{2+}$  signaling in starfish oocytes, we have found that many aspects of the intracellular  $\text{Ca}^{2+}$  increases in the oocytes undergoing meiotic maturation, as well as in the eggs fertilized or microinjected with the second messengers, were significantly influenced by the actin cytoskeleton. This has been demonstrated in various approaches by microinjecting the actin-binding protein cofilin [12], the function-blocking antibody against depactin [13], inhibitor of G-protein [14], or the PIP2-sequestering domain of PLC- $\delta$ 1 [15], each of which changes the state of the actin cytoskeleton by directly or indirectly altering the activity or availability of the actin-binding proteins, as well as by using actin-binding drugs [16,17]. In these studies with starfish eggs, we have demonstrated that the actin cytoskeleton plays comprehensive roles at fertilization by modulating not only  $\text{Ca}^{2+}$  signaling, but also cortical granules exocytosis and sperm entry.

In one striking case, incubation of the eggs from a certain species of starfish (*Astropecten aranciatus*) with an actin-binding drug latrunculin A (LAT-A) caused a ‘spontaneous’ rise of intracellular  $\text{Ca}^{2+}$  waves without an aid of exogenous factors such as sperm or second messengers [18], but this extraordinary phenomenon has not been observed in the eggs of other echinoderm species. Thus, the aforementioned roles of the actin cytoskeleton might be restricted to a certain species of echinoderm, and herein we have tested whether or not those effects that we had observed in the fertilized eggs of starfish could be also demonstrated with sea urchin eggs. To this end, we have used two different actin-binding drugs that promote net depolymerization of actin (cytochalasin B and latrunculin A) and two others that rather stabilize actin filaments (jasplakinolide and phalloidin), and their effects on the pattern of  $\text{Ca}^{2+}$  signaling, cortical granules exocytosis, and sperm entry were compared in one place.

## 2. Materials and methods

### 2.1. Preparation of gametes

Adult animals of sea urchin (*Paracentrotus lividus*) were captured from the Gulf of Naples during the breeding season, and kept in the circulating seawater (16 °C). Eggs were collected from females by an intracoelomic injection of 0.5 M KCl, and dry sperm were surgically removed from the male gonad. Fertilization was performed at  $3.7 \times 10^6$  spermatozoa/ml (final density) in fresh seawater. To determine the number of egg-incorporated spermatozoa, sperm were stained with Hoechst 33342 (Sigma–Aldrich) as described previously [19].

### 2.2. Microinjection, confocal microscopy, and video imaging

The method of microinjection regarding injection buffer, trans-jector, and volumetric calibration was previously described in detail [15,19]. Fresh intact eggs were microinjected with a gentle tapping of the apparatus without additional steps of removing jelly coats. For  $\text{Ca}^{2+}$  imaging, Calcium Green 488 conjugated to 10 kD dextran (500  $\mu\text{M}$ ) was mixed with Rhodamine Red (35  $\mu\text{M}$ ) in the injection buffer. To visualize F-actin in a living egg, 10  $\mu\text{M}$  AlexaFluor568–phalloidin was injected into eggs as previously described [17], and the eggs were monitored with a CrEST X-Light spinning disk confocal microscope. The bright field view and the fluorescence images of  $\text{Ca}^{2+}$  were detected with a cooled CCD camera (MicroMax, Princeton Instruments, Inc) in about 2 s time resolution, and were analyzed with MetaMorph (Universal Imaging Corporation). The quantified  $\text{Ca}^{2+}$  signal at a given time point was normalized to the baseline fluorescence ( $F_0$ ) following the formula  $F_{\text{rel}} = [F - F_0]/F_0$ , where  $F$  represents the average fluorescence level of the entire egg. Thus,  $F_{\text{rel}}$  was defined as RFU (relative fluorescence unit) for plotting  $\text{Ca}^{2+}$  trajectories in Figs. 2 and 3. To compensate batch-to-batch variability of  $\text{Ca}^{2+}$  signals, the peak amplitudes of the  $\text{Ca}^{2+}$  wave and the cortical flash of each egg were normalized with the averages of the corresponding values in the control eggs from the same batch. Thus, the data presented in reference to the batch-matching control (taken as 100%) was pooled together and subjected to statistical analyses. To visualize the momentary increase of  $\text{Ca}^{2+}$  signals in subcellular regions, incremental changes of the  $\text{Ca}^{2+}$  rise were analyzed by applying the formula  $F_{\text{inst}} = [(F_t - F_{t-1})/F_{t-1}]$  and used for illustrations in Figs. 2 and 3 (top panels).

### 2.3. Chemicals and statistical analysis

All fluorescent probes and the actin-binding drugs, except phalloidin (Sigma–Aldrich), were purchased from Molecular Probes.

The average and variation of the data were reported as ‘mean  $\pm$  SD (standard deviation)’ in all cases. The paired and unpaired  $t$ -tests and the one-way ANOVA were performed by use of Prism 3.0 (GraphPad Software, La Jolla, USA), and the  $P$ -values smaller than 0.05 ( $P < 0.05$ ) were considered statistically significant.

## 3. Results

### 3.1. Effects of the actin-binding drugs on structure dynamics of the actin cytoskeleton in sea urchin eggs

The actin cytoskeleton is a dynamical structure that undergoes constant changes even in a quiescent egg. Thus, actin-binding drugs are expected to cause structural changes to the actin cytoskeleton by interfering with the natural process of treadmilling. To demonstrate the efficacy of the actin-binding drugs and to compare their effects on the structure of the actin cytoskeleton in sea urchin eggs, we microinjected individual eggs with a small amount of AlexaFluor568–phalloidin that does not interfere with biological processes by itself [15,17]. Five minutes later, the eggs were treated with the four different actin-binding drugs or their vehicles as a control, and the structural changes of the actin cytoskeleton in the living eggs were monitored by confocal microscopy at five minutes’ intervals. As shown in Fig. 1A, the control eggs treated with 0.4% DMSO retained a myriad of fluorescently stained actin filaments in the cytoplasm over the 20 min period. However, in the eggs treated with 2  $\mu\text{M}$  cytochalasin B (CYT-B), the actin filaments began to disappear at 5 min and were hardly visible in the cytoplasm by 15 min. Likewise, the eggs treated with 3  $\mu\text{M}$  latrunculin A (LAT-A) displayed reduction of the heavily labeled actin filaments by 5 min, but some of them lingered on in the cytoplasm for the 20 min period. Nonetheless, the actin cytoskeleton in these eggs appeared to be globally altered, as judged by the loss of the perfectly spherical cell shape by 5 min, which reflects a substantial change in cell rigidity. In contrast to CYT-B and LAT-A that tended to shift actin filaments towards net depolymerization, the other two drugs known to stabilize actin filaments strongly enhanced the actin meshwork underneath the plasma membrane. In the eggs exposed to 12  $\mu\text{M}$  jasplakinolide (JAS), the layer of the subplasmalemmal actin filaments became visibly thicker by 5 min (Fig. 1A, arrow). Likewise, the eggs microinjected with 1 mM phalloidin (PHAL) exhibited intense hyperpolymerization of actin in the subplasmalemmal region of the cortex by 5 min (Fig. 1B, arrow), with the concomitant depolymerization in the inner cytoplasm. Thus, all the four actin drugs at given doses displayed appreciable structural changes in the actin cytoskeleton in specific subcellular regions.

### 3.2. Effects of cytochalasin B and latrunculin A on the intracellular $\text{Ca}^{2+}$ increase in the sea urchin eggs responding to fertilizing sperm

We then examined how fertilization is affected by the two actin-binding drugs that promote net depolymerization. First, we monitored their effects on the  $\text{Ca}^{2+}$  response at fertilization. As shown in Fig. 2, CYT-B and LAT-A exhibited similar effects in many aspects. The most conspicuous thing about the  $\text{Ca}^{2+}$  response in the eggs pretreated with CYT-B (2  $\mu\text{M}$ , 10 min) was that the time interval between the cortical flash and the detection of the first  $\text{Ca}^{2+}$  spot at the sperm interaction site, which was defined as the ‘latent period’ in this work, was distinctively increased ( $12.3 \pm 4.9$  s,  $n = 47$ ) in comparison with the control eggs ( $7.8 \pm 3.3$  s,  $n = 36$ ;  $P < 0.0001$ ), although the amplitude of the cortical flash itself remained virtually unchanged:  $111.0 \pm 30.8\%$  in CYT-B-pretreated eggs vs.  $100.0 \pm 19.4\%$  in the control eggs treated with 0.1% DMSO,  $P = 0.2223$  (Fig. 2A). Likewise, the latent period in the eggs

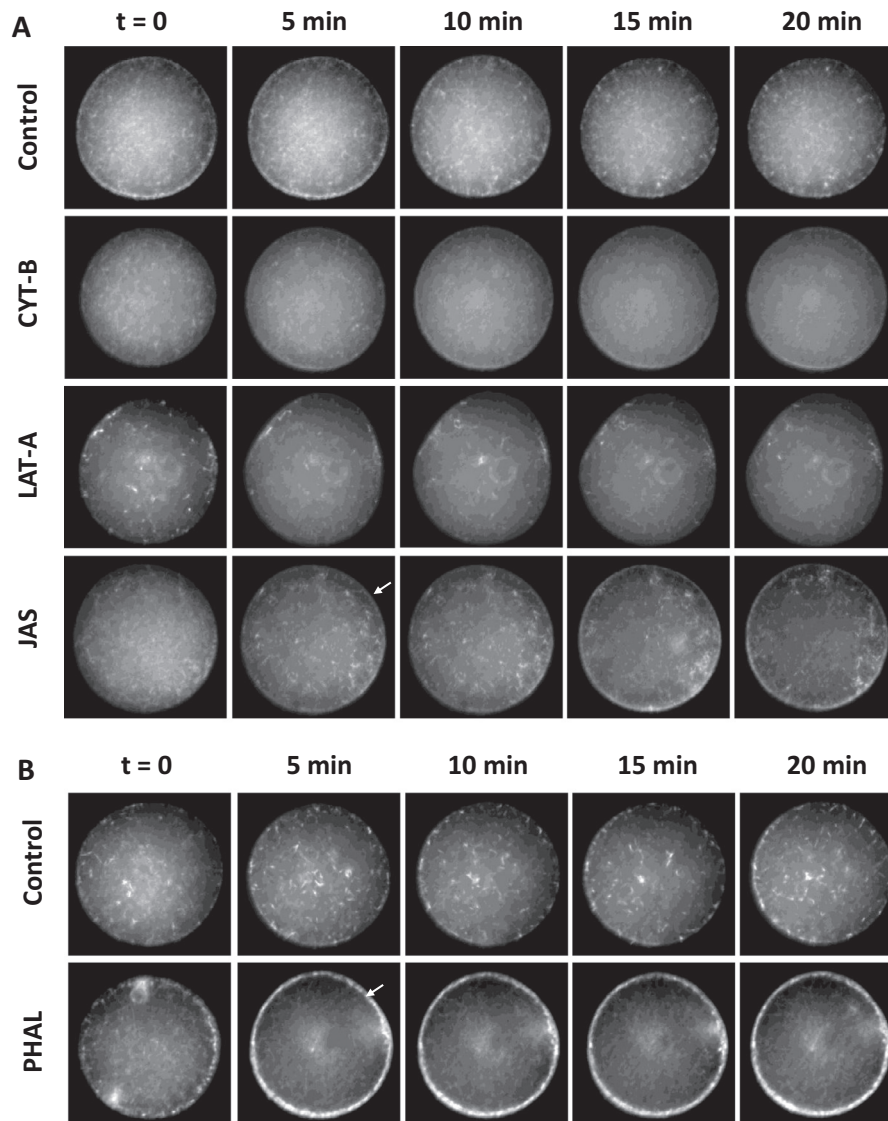


**Fig. 1.** Alteration of the actin cytoskeleton in the sea urchin eggs treated with the actin-binding drugs. *P. lividus* eggs were microinjected with AlexaFluor568–phalloidin (10  $\mu$ M in pipette) and subsequently treated with four different actin-binding drugs to compare their effects. (A) The eggs loaded with the fluorescent probe for F-actin were then incubated in seawater containing either 0.4% DMSO (control) or one of the actin-binding drugs: CYT-B (2  $\mu$ M cytochalasin B), LAT-A (3  $\mu$ M latrunculin A), and JAS (12  $\mu$ M jasplakinolide). For each treatment, the moment immediately before drug addition was taken as  $t = 0$ , and the time-lapse images of the actin cytoskeleton were obtained with confocal microscopy at the equatorial plane. (B) Being membrane-impermeant, phalloidin (PHAL, 1 mM in pipette) was delivered to the eggs by a second microinjection after 10 min recovery, whereas the control eggs were microinjected with DMSO. Arrows indicate the subplasmalemmal layer where actin was readily hyperpolymerized following the treatment.

pretreated with LAT-A (100 nM, 15 min) was also significantly increased ( $9.1 \pm 2.6$  s,  $n = 18$ ) in comparison with the control ( $7.4 \pm 2.5$  s,  $n = 22$ ;  $P < 0.01$ ). The amplitude of the cortical flash in these eggs displayed high variability, but was not significantly different from that of the control ( $90.9 \pm 56.0\%$  vs.  $100.0 \pm 22.2\%$ ;  $P = 0.4400$ ) (Fig. 2B). On the other hand, the peak amplitude of the global  $\text{Ca}^{2+}$  increase was significantly decreased in both cases. The  $\text{Ca}^{2+}$  peak in the CYT-B-pretreated eggs scored  $90.8 \pm 22.0\%$  ( $n = 47$ ,  $P < 0.05$ ) of the level in the control ( $100.0 \pm 11.4\%$ ,  $n = 36$ ), and the  $\text{Ca}^{2+}$  peak in the LAT-A-pretreated eggs was merely  $74.1 \pm 14.8\%$  ( $n = 18$ ,  $P < 0.0001$ ) of the level in the control eggs ( $100.0 \pm 14.6\%$ ,  $n = 22$ ). Another remarkable observation in the eggs pretreated with LAT-A was that the  $\text{Ca}^{2+}$  wave initiating at the sperm interaction site failed to propagate to the antipode in 72.2% of the cases ( $n = 18$ ), whereas the  $\text{Ca}^{2+}$  wave in the control egg always displayed complete propagation ( $n = 22$ ). The LAT-A-pretreated eggs often displayed irregular  $\text{Ca}^{2+}$  increases that

had apparently initiated at multiple sites but faded out before being developed as a coordinated wave (Fig. 2B, red arrowheads). In addition to these localized erratic  $\text{Ca}^{2+}$  increases, insemination of the LAT-A-pretreated eggs led to production of multiple  $\text{Ca}^{2+}$  peaks on a larger time scale, which usually started at different areas of the egg surface and developed into at least a partial wave (Fig. 2B,  $\text{Ca}^{2+}$  trajectories in bold lines). To a lesser extent, the  $\text{Ca}^{2+}$  wave in the CYT-B-pretreated eggs failed to reach the antipode in 23.4% of the cases ( $n = 47$ ). Interestingly, even in cases where a  $\text{Ca}^{2+}$  wave successfully traversed the CYT-B-pretreated eggs, the time span from the initial  $\text{Ca}^{2+}$  spot to the fading one in the antipode (defined here as the ‘traverse time’) was significantly increased ( $22.3 \pm 4.4$  s,  $n = 36$ ) in comparison with that in the control ( $17.8 \pm 3.1$  s,  $n = 35$ ;  $P < 0.0001$ ). Accordingly, the planar speed of the  $\text{Ca}^{2+}$  wave was significantly reduced in the CYT-B-treated eggs (circa 3.6  $\mu\text{m/s}$ , as opposed to 4.5  $\mu\text{m/s}$  in the control). To a lesser degree, the traverse time of the  $\text{Ca}^{2+}$  wave in

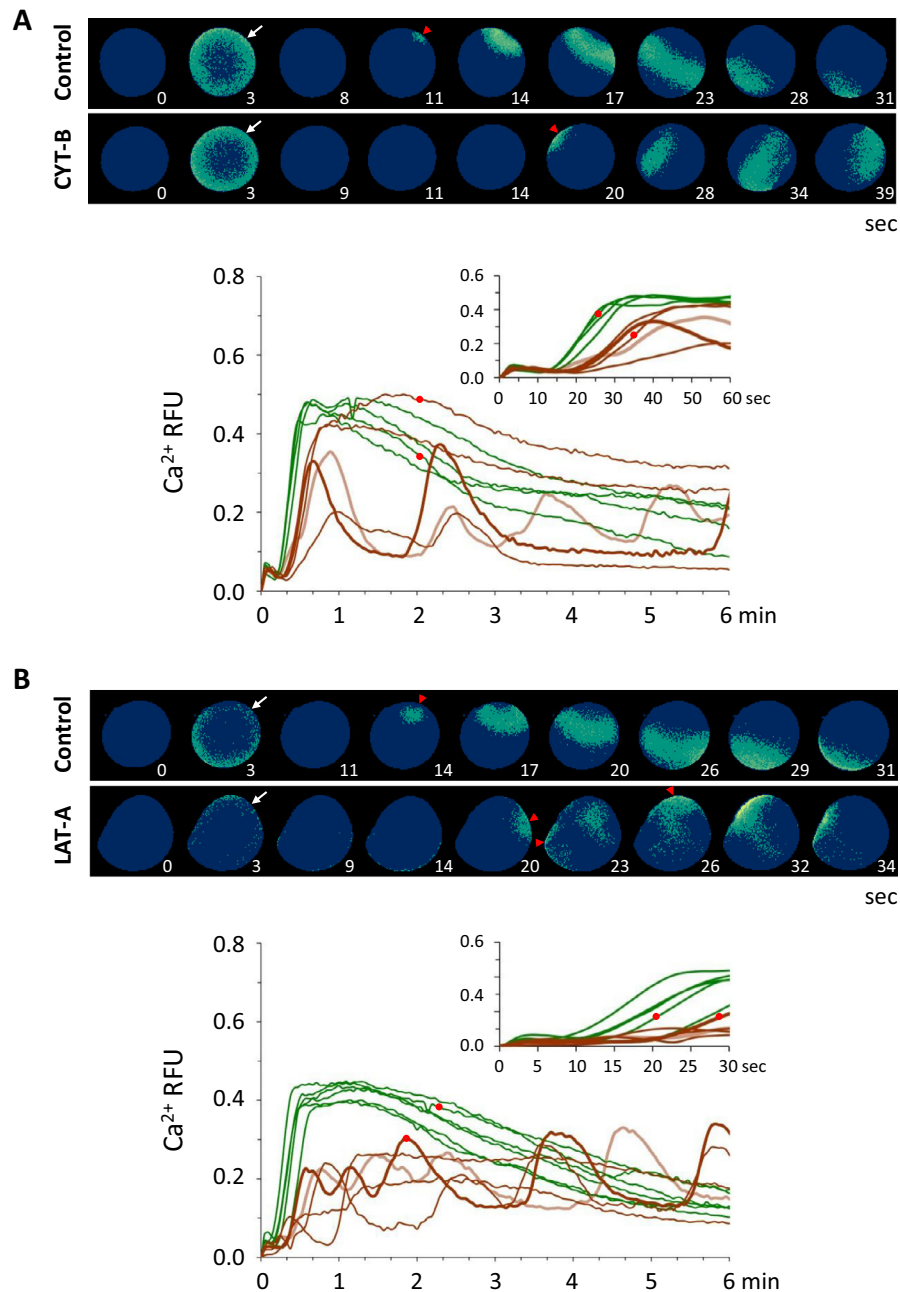


**Fig. 2.** Effects of cytochalasin B and latrunculin A on the intracellular  $\text{Ca}^{2+}$  increase in the sea urchin eggs responding to fertilizing sperm. (A) *P. lividus* eggs were microinjected with calcium dyes and incubated in seawater containing 2  $\mu\text{M}$  CYT-B or 0.1% DMSO (control). Ten minutes later, the eggs were thoroughly rinsed and inseminated in fresh seawater. The changes of the intracellular  $\text{Ca}^{2+}$  level were monitored after sperm addition in the control (green curves) and CYT-B-pretreated eggs (brown curves). The pseudo-colored relative fluorescence images at the top represent the sites of momentary  $\text{Ca}^{2+}$  increases at the key time points (numbers refer to 'seconds' after  $t = 0$ ), and the  $\text{Ca}^{2+}$  trajectories in the graph trace the global changes of the  $\text{Ca}^{2+}$  levels in reference to the background. In this and other figures, the time frame immediately before the first detectable  $\text{Ca}^{2+}$  signal in the CCD camera recording was set to time zero ( $t = 0$ ). Here, results from one of the five independent experiments were illustrated. For visual distinction, two  $\text{Ca}^{2+}$  trajectories displaying repetitive patterns were marked with bold lines with different shades. In the inset is the same  $\text{Ca}^{2+}$  trajectories plotted on a different time scale to depict the initial  $\text{Ca}^{2+}$  changes. The cortical flash and the initial  $\text{Ca}^{2+}$  spots at the presumed sites of significant sperm contact were marked by arrows and arrowheads, respectively. (B) Results of a comparable experiment with the 15 min pretreatment with 100 nM LAT-A or 0.1% DMSO (control). Out of three independent experiments, data from one representative batch of eggs were presented here. The  $\text{Ca}^{2+}$  trajectories of the eggs whose  $\text{Ca}^{2+}$  waves were visualized in panel A were marked with small red circles.

the LAT-A-pretreated eggs was also increased ( $20.0 \pm 5.3$  s,  $n = 5$ ), but its difference from the values in the control ( $18.2 \pm 2.2$  s,  $n = 22$ ) did not reach statistical significance. Overall, the eggs pretreated with CYT-B or LAT-A shared similarities in nearly all aspects of the  $\text{Ca}^{2+}$  response at fertilization (Fig. 2) in agreement with their comparable effects on the morphology of the actin cytoskeleton (Fig. 1).

### 3.3. Effects of jasplakinolide and phalloidin on the intracellular $\text{Ca}^{2+}$ increase in the sea urchin eggs responding to fertilizing sperm

We then examined how fertilization of sea urchin eggs would be affected by the other class of actin drugs, i.e. JAS and PHAL, which tended to stabilize actin filaments in the subplasmalemmal regions (Fig. 1). Unlike the cases with CYT-B and LAT-A, the eggs



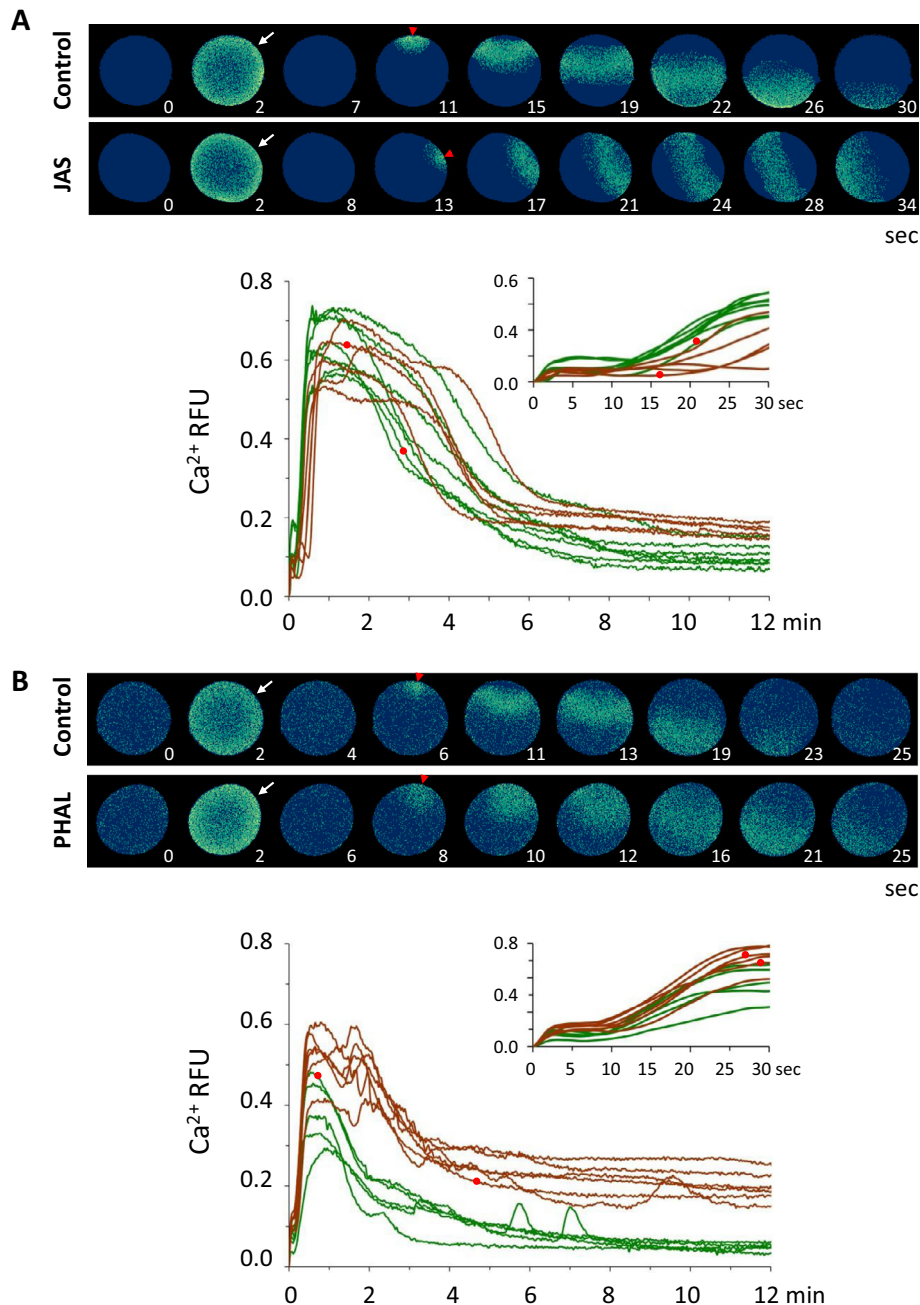


**Fig. 3.** Effects of jasplakinolide and phalloidin on the intracellular  $\text{Ca}^{2+}$  increase in the sea urchin eggs responding to fertilizing sperm. (A) *P. lividus* eggs were microinjected with calcium dyes and incubated in seawater containing 12  $\mu\text{M}$  JAS or 0.4% DMSO (control). Twenty minutes later, the eggs were extensively rinsed in fresh seawater and sperm were added. The changes of the intracellular  $\text{Ca}^{2+}$  level were monitored after sperm addition in the control (green curves) and JAS-pretreated eggs (brown curves), and presented in pseudo-colored relative fluorescence images and in  $\text{Ca}^{2+}$  trajectory graphs, as described in the legend of Fig. 2. Results from one of the three independent experiments were illustrated. (B) *P. lividus* eggs were microinjected with the calcium dye mixed with either 1 mM PHAL (concentration in the pipette) or DMSO (control). After 20 min incubation, the eggs were inseminated, and the  $\text{Ca}^{2+}$  response was monitored and presented as described in the legend of Fig. 2. The  $\text{Ca}^{2+}$  trajectories in the control and the PHAL-microinjected eggs were depicted in green and brown curves, respectively. Data from one of the four independent experiments were presented here.

treated with JAS (12  $\mu\text{M}$ , 20 min) or microinjected with 1 mM PHAL (20 min incubation) displayed no significant difference from their control eggs with respect to the latent period. JAS-pretreated eggs scored  $8.8 \pm 4.0$  s ( $n = 24$ ) which was similar to  $8.1 \pm 1.7$  s of the control eggs exposed to 0.4% DMSO ( $n = 22$ ,  $P = 0.2485$ ). PHAL-injected eggs also scored  $7.5 \pm 2.4$  s ( $n = 29$ ) which was not much different from  $7.0 \pm 1.3$  s of the DMSO-injected control eggs ( $n = 24$ ,  $P = 0.3975$ ) (Fig. 2). However, these two drugs had significant effects on the cortical flash, but in opposite ways. Whereas JAS slightly repressed the amplitude of the cortical flash ( $82.9 \pm 22.3\%$

vs.  $100 \pm 22.5\%$  of the level in the control,  $P < 0.05$ ), PHAL strongly enhanced it ( $162.7 \pm 100.3\%$  vs.  $100 \pm 27.6\%$  of the level in the control,  $P < 0.01$ ). As to the global  $\text{Ca}^{2+}$  increase at fertilization, pretreatment of sea urchin eggs with JAS did not make a significant difference to the peak amplitude, which was  $90.6 \pm 23.8\%$  of the level in the control ( $100 \pm 19.4\%$ ,  $P = 0.2142$ ) (Fig. 3A). At variance with this, the  $\text{Ca}^{2+}$  peak in the eggs preinjected with 1 mM PHAL ( $n = 30$ ) exhibited a strong enhancement:  $140.6 \pm 59.3\%$  in comparison with the control,  $100.0 \pm 13.3\%$  ( $n = 26$ ,  $P < 0.01$ ) (Fig. 3B). Despite these subtle differences, however, the pretreatment of

sea urchin eggs with JAS or PHAL manifested strikingly similar effects at the phase of  $\text{Ca}^{2+}$  decay. Whereas the  $\text{Ca}^{2+}$  signals in the entire field of the DMSO-treated control eggs continued to decline after the peak (Fig. 3A and B, green curves), the diminishing  $\text{Ca}^{2+}$  levels in the JAS- and PHAL-treated eggs apparently came to a virtual halt at about 5 and 3 min, respectively (Fig. 3A and B, brown curves). As a result, the fading  $\text{Ca}^{2+}$  signals in these eggs arrived at a plateau, which was distinctively higher than the  $\text{Ca}^{2+}$  trajectories of their corresponding control eggs. To quantify this, we extrapolated the two linear stretches of the declining  $\text{Ca}^{2+}$  trajectories before and after the sharp curvature at the beginning of the plateau, and obtained the  $\text{Ca}^{2+}$  level at the crossing time point and normalized it with the amplitude of the  $\text{Ca}^{2+}$  peak. The ratio of plateau to peak thus defined was significantly higher in the eggs pretreated with JAS ( $0.406 \pm 0.086$ ,  $n = 17$ ) than in the control eggs ( $0.175 \pm 0.039$ ,  $n = 22$ ;  $P < 0.0001$ ), as well as in the PHAL-preinjected eggs ( $0.455 \pm 0.089$ ,  $n = 30$ ) in comparison with their control eggs ( $0.231 \pm 0.102$ ,  $n = 26$ ;  $P < 0.0001$ ). Hence, it appeared that the  $\text{Ca}^{2+}$  ions mobilized at fertilization was reabsorbed from cytosol with much less efficiency or capacity in those eggs that had been pretreated with the drugs inducing actin hyperpolymerization in the cortex and subplasmalemmal regions.

#### 3.4. Effects of the actin-binding drugs on sperm entry and elevation of the fertilization envelope

In normal experimental conditions, insemination of *P. lividus* eggs almost always leads to monospermic fertilization [20] and full elevation of the fertilization envelope (FE), the latter of which results from cortical granules exocytosis. We tested whether the sperm entry and FE elevation would be influenced by actin-binding drugs in a dose-dependent manner. To this end, *P. lividus* eggs pretreated with increasing concentrations of actin drugs were extensively rinsed and inseminated with Hoechst 33342-stained sperm. The number of egg-incorporated sperm was then scored in each egg (Fig. 4A), and the frequency of the eggs displaying full elevation of the FE at each drug dose was averaged from the results of 4–6 independent experiments comprising 20–40 eggs. As shown in Fig. 4B (brown dots and lines), the average percentage of the eggs displaying full elevation of the FE dropped progressively with the increasing doses of the four actin-binding drugs. In parallel, the number of the egg-incorporated sperm also diminished (Fig. 4B, green bars), suggesting that the four actin-drugs pre-administered to the eggs generally inhibited sperm entry. However, we noted that a lower dose of CYT-B ( $0.4 \mu\text{M}$ , 10 min) contrarily increased the number of egg-incorporated sperm ( $1.2 \pm 0.51$  per egg,  $n = 60$ ) in comparison with the control eggs ( $1.03 \pm 0.18$  per egg,  $n = 87$ ;  $P < 0.01$ ). This small but significant increase of polyspermy in the CYT-B-pretreated eggs cannot be attributed to the incomplete elevation of the FE, as all the eggs displaying polyspermy (9 out of 60) incorporated 2–3 sperm in the face of full elevation of the FE (Fig. 4A, see the three internalized sperm in a CYT-B-pretreated egg). Conversely, all the eggs that exhibited incomplete elevation of the FE (14 out of 60) ended up with monospermic fertilization. A similar trend of increased polyspermy at a low dose was also found in the eggs microinjected with PHAL ( $3 \mu\text{M}$ , estimated concentration in cytosol), which scored  $1.31 \pm 1.27$  sperm per egg ( $n = 80$ ,  $P < 0.05$ ) as opposed to  $1.01 \pm 0.11$  ( $n = 80$ ) for the control eggs microinjected with DMSO (Fig. 4B, PHAL). It is noteworthy that PHAL was administered to the eggs by microinjection unlike the other three drugs, which were added by bath incubation, and that the microinjection of the vehicle itself (DMSO) significantly lowered the frequency of the eggs displaying full elevation of the FE (only  $80.0 \pm 24.8\%$ ,  $N = 4$ ). Nonetheless, only 1 out of 80 DMSO-microinjected eggs

exhibited entry of multiple sperm, suggesting that the presence or absence of a fully elevated FE is not the major determinant of polyspermy in sea urchin eggs. Despite the lack of the mechanical barrier and apparent adherence of the sperm (Fig. 4A), the eggs pretreated with the highest given doses of the four actin-binding drugs were able to incorporate sperm only scarcely, as the average number of egg-incorporated sperm was drastically reduced in the eggs pretreated with CYT-B ( $0.05 \pm 0.22$ ,  $n = 60$ ), LAT-A ( $0.11 \pm 0.34$ ,  $n = 120$ ), JAS ( $0.0 \pm 0.0$ ,  $n = 60$ ), and PHAL ( $0.013 \pm 0.11$ ,  $n = 80$ ) in comparison with their corresponding control eggs ( $P < 0.0001$  in all cases) (Fig. 4B). Taken together, these results indicated that the actin-binding drugs used in this study had dose-dependent effects on sperm entry. At higher doses, they commonly inhibited the sperm incorporation mechanism of the egg; but at low doses, CYT-B and PHAL increased incidents of supernumerary sperm entry.

#### 4. Discussion

In this communication, we have reported that the actin-binding drugs pre-administered to sea urchin eggs have profound effects on  $\text{Ca}^{2+}$  signaling, cortical granules exocytosis, and sperm entry at fertilization. Sea urchin eggs pretreated with CYT-B or LAT-A, which generally promotes net depolymerization of cortical actin (Fig. 1), manifested several common features of  $\text{Ca}^{2+}$  increases at fertilization. First, the time span between the cortical flash and the onset of the first detectable  $\text{Ca}^{2+}$  spot at the sperm interaction site (the 'latent period') was significantly prolonged by 57% and 23% when the eggs were pretreated with CYT-B and LAT-A (Fig. 2). Although much lower in time resolution, our results are in line with the previous electrophysiological data reporting that the interval between the step potential and the fertilization potential increased nearly twofold by cytochalasin [21]. Thus, the cortical flash and the initial  $\text{Ca}^{2+}$  spot at the sperm interaction site may correspond to the step potential and the onset of the fertilization potential, respectively. However, the exact physiological significance of the latent period and its prolongation by cytochalasin is not clear [21,22]. In view of the historical theories on how sperm activates the eggs [9,23,24], the latent period may reflect the time needed by the successful sperm either to physically infuse a substance into the egg via a conduit or to transmit a cascade of signals through a receptor on the egg surface. Whichever may be the pathway, CYT-B and LAT-A appeared to delay it significantly (Fig. 2). Thus, the egg subplasmalemmal actin cytoskeleton is thought to be implicated in this yet unclear process that leads from sperm interaction to the generation of the initial  $\text{Ca}^{2+}$  spot.

The other characteristic feature often found in the eggs pretreated with CYT-B or LAT-A was the generation of multiple  $\text{Ca}^{2+}$  peaks at fertilization (Fig. 2). During the first 6 min of the  $\text{Ca}^{2+}$  response, the LAT-A-pretreated eggs exhibited as many as  $3.8 \pm 2.1$  peaks ( $n = 18$ ) in comparison with their control eggs ( $1.05 \pm 0.21$ ,  $n = 22$ ;  $P < 0.0001$ ). To a lesser extent, the CYT-B-pretreated eggs displayed  $1.8 \pm 0.95$  ( $n = 47$ )  $\text{Ca}^{2+}$  peaks in the same period, as opposed to  $1.19 \pm 0.47$  scored by the control eggs ( $n = 36$ ,  $P < 0.01$ ). The occurrence of the multiple  $\text{Ca}^{2+}$  peaks at fertilization was extremely sensitive to LAT-A, as the minimal dose to induce the phenomenon was as low as 1 nM. This supernumerary  $\text{Ca}^{2+}$  increases facilitated by LAT-A was somewhat reminiscent of the 'spontaneous'  $\text{Ca}^{2+}$  increase in *A. aranciacus* eggs bathed in the presence of LAT-A [18], but was clearly different from it. First, LAT-A alone could not induce  $\text{Ca}^{2+}$  increase without sperm in *P. lividus* eggs, and the similar experiment with LAT-A and a  $\text{Ca}^{2+}$ -ionophore produced only a single  $\text{Ca}^{2+}$  peak (data not shown). Thus, the multiple  $\text{Ca}^{2+}$  increase that usually start from different areas of the egg surface and develop into a partial wave are likely to represent multiple sperm interaction. Nonetheless, in the same

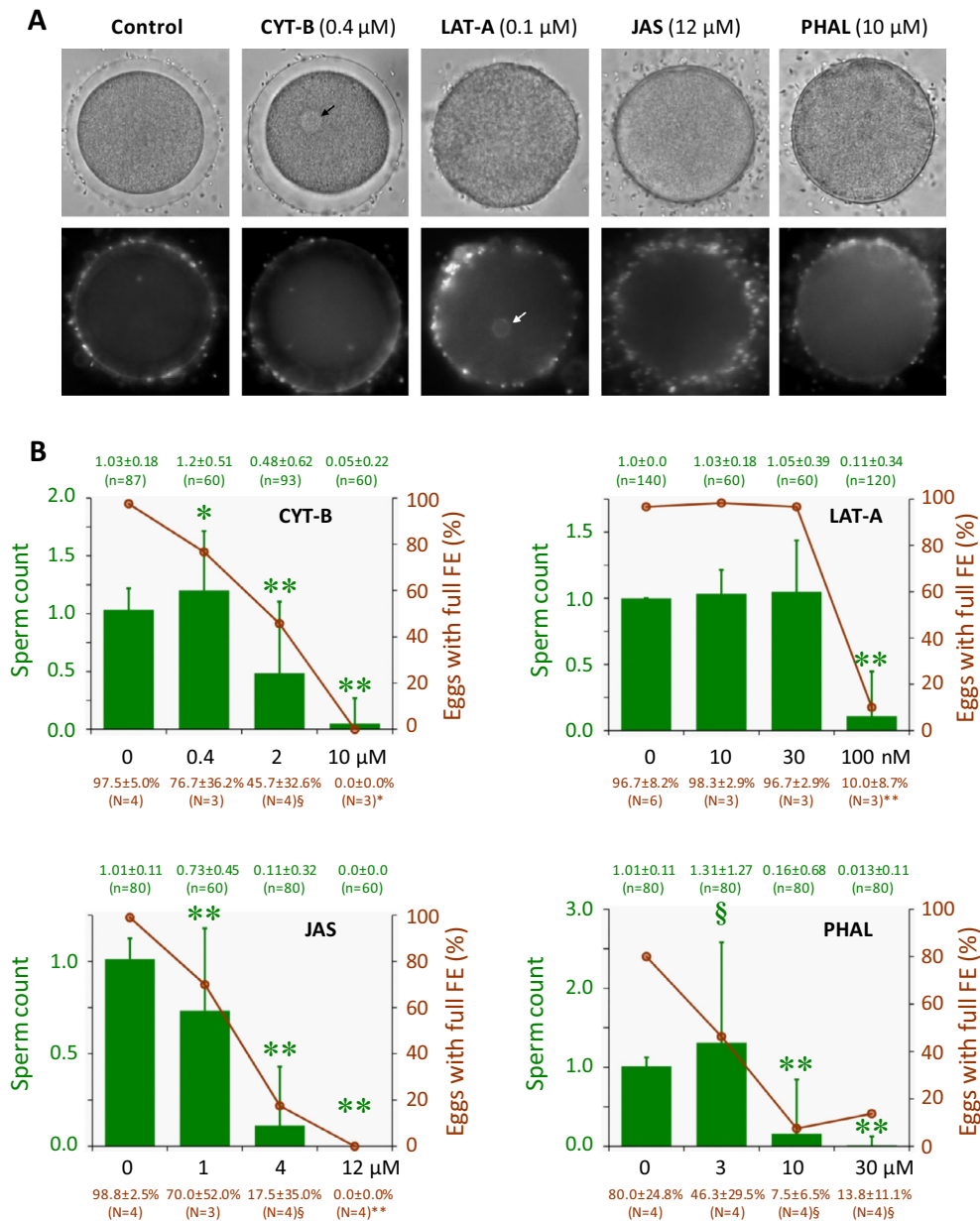


**Fig. 4.** Effects of the actin-binding drugs on sperm entry and elevation of the fertilization envelope. *P. lividus* eggs were treated with increasing doses of the actin-binding drugs and inseminated with Hoechst 33342-stained sperm, and their effects on fertilization was monitored by assessing the number of egg-incorporated sperm and the percentage of the eggs displaying full elevation of the FE. Incubation time: CYT-B, 10 min; LAT-A, 15 min; JAS, 20 min; PHAL, 20 min. (A) About 5 min after insemination, the elevation of the FE and the number of egg-incorporated sperm were respectively examined in the bright field view (top) and in epifluorescence microscopy (bottom). Arrows indicate egg pronuclei that happened to be in focus. (B) Graphic summaries of the dose-dependent effects of the actin-binding drugs on fertilization. The average frequency of the eggs displaying full elevation of the FE was presented in brown dots and lines, and the exact Mean  $\pm$  SD and the number (N) of independent batches were indicated below the corresponding drug concentration. The average number of egg-incorporated sperm was calculated from the pooled data at the given dose of each drug, and was presented in green histogram. The exact Mean  $\pm$  SD and the number of the eggs examined (n) were indicated above the corresponding bars of the histogram. The results indicating a significant difference from the values in the control were marked with special symbols: § $P$  < 0.05, \* $P$  < 0.01, \*\* $P$  < 0.0001.

condition (100 nM LAT-A, 15 min), the eggs were hardly entered by spermatozoa (Fig. 4B).

The occurrence of the multiple  $\text{Ca}^{2+}$  peaks evoked by spermatozoa was not restricted to the eggs pretreated with actin-depolymerization drugs. We found that the eggs pretreated with JAS also produced  $1.63 \pm 1.10$   $\text{Ca}^{2+}$  peaks ( $n = 24$ ), as opposed to  $1.05 \pm 0.21$  peaks manifested by the control eggs ( $n = 22$ ,  $P < 0.05$ ). A similar trend was also observed in the PHAL-preinjected eggs ( $1.40 \pm 0.56$ ,  $n = 30$ ) but the difference from the values in the DMSO-preinjected control eggs did not reach statistically significance ( $1.23 \pm 0.51$ ,  $n = 26$ ;  $P = 0.2026$ ). Thus, it appeared that

the eggs pretreated with actin drugs were more permissive toward spermatozoa and let them trigger  $\text{Ca}^{2+}$  waves from multiple sites.

Although the global  $\text{Ca}^{2+}$  wave in the JAS-pretreated eggs was highly comparable to that of the control eggs in terms of its amplitude (Fig. 3A), the eggs treated in the same condition (12  $\mu$ M, 20 min) was hardly entered by spermatozoa (Fig. 4B), whereas eggs displaying a single  $\text{Ca}^{2+}$  peak could occasionally incorporate multiple sperm (data not shown). Thus, an episode of  $\text{Ca}^{2+}$  wave at fertilization is neither necessary nor sufficient for individual sperm entry in sea urchin eggs, while the structural or functional status of the egg actin cytoskeleton was closely linked to the sperm

entry (Fig. 4). The universal failure at incorporating sperm displayed by the eggs pretreated with the actin drugs was not attributable to a potentially deleterious effect of the drugs on sperm motility because non-pretreated control eggs present in the same chamber were successfully fertilized amid the failing actin drug-pretreated eggs (data not shown).

The entry of supernumerary sperm in the eggs exhibiting normal elevation of the FE, together with the lack of sperm entry in the eggs with no FE elevation (Fig. 4A), implies that the formation of the FE might be of no practical service towards block to polyspermy [25]. Hence, monospermic fertilization in sea urchin eggs may be assured by a faster mechanism, as was first suggested by E.E. Just [20] and later postulated on the basis of a rapid depolarization of the egg membrane potential at fertilization [26]. While the exact mechanism of a fast block to polyspermy is still on the debate as was discussed in this issue [27] and elsewhere [28], the results of our study indicated that the exquisite coordination of the actin cytoskeleton is a prerequisite for proper sperm interaction (multiple  $\text{Ca}^{2+}$  peaks in LAT-A- and CYT-B-pretreated eggs) and incorporation, which might lead to regulation of a mechanism ensuring monospermic sperm entry (Fig. 4). In support of the idea that the actin cytoskeleton plays a dominating role in the control of monospermy independent of the FE, it was demonstrated that surf clam eggs, which do not substantially elevate the FE, became highly polyspermic at fertilization when they were pretreated with CYT-B [29].

Another important point in our study was that the JAS-pretreated eggs succeeded to elevate the FE in none of the 60 eggs examined (Fig. 4), although the same experimental condition (12  $\mu\text{M}$ , 20 min) still produced a massive  $\text{Ca}^{2+}$  wave that is comparable with the control eggs (Fig. 3A). All other drugs manifested basically the same phenomena: a failure of triggering cortical granules exocytosis despite the fact that the cytosolic  $\text{Ca}^{2+}$  increase physically took place. Hence, it is evident that the increase of  $\text{Ca}^{2+}$  alone was not sufficient for the exocytosis of cortical granules at fertilization, but instead required an exquisite cooperation of the actin cytoskeleton, which corroborated our previous findings from starfish eggs [15–17,19].

In addressing general effects of the actin-binding drugs on the egg's  $\text{Ca}^{2+}$  response at fertilization, the amplitude of the cortical flash, which reflects the  $\text{Ca}^{2+}$  influx via voltage-gated  $\text{Ca}^{2+}$  channel, was selectively affected by the drugs stabilizing actin filaments (Fig. 3). On the other hand, the peak amplitude of the global  $\text{Ca}^{2+}$  wave was moderately repressed in the eggs pretreated with CYT-B and LAT-A by 9% and 26%, respectively, but was enhanced by 41% in PHAL-pretreated eggs. In contrast to PHAL, the JAS-pretreated eggs displayed virtually no significant changes in the peak amplitude of the  $\text{Ca}^{2+}$  waves in comparison with their control eggs (Fig. 3). These subtle differences between JAS and PHAL in their effects on  $\text{Ca}^{2+}$  signaling peak are difficult to explain since their exact influences on the actin filaments in specific subcellular loci around endoplasmic reticulum (ER) and in microvilli are largely unknown. Nonetheless, we found that both JAS and PHAL had a similar effect at the decay phase of the  $\text{Ca}^{2+}$  trajectories (Fig. 3). After being released from the stores,  $\text{Ca}^{2+}$  ions are to be buffered by  $\text{Ca}^{2+}$ -binding proteins or reabsorbed back to the intracellular stores, or even pumped out of the cell. Thus, after reaching the peak, the net  $\text{Ca}^{2+}$  mobilization is toward buffering or reuptake into the source, but we intriguingly found that the removal of the cytosolic  $\text{Ca}^{2+}$  came to an earlier saturation in the eggs pretreated with JAS and PHAL (Fig. 3). This phenomenon was not found in the eggs pretreated with actin-depolymerizing drugs, but was more evident in the eggs pretreated with PHAL (Fig. 3B) that displayed stronger hyperpolymerizing effects on the cortical actin (Fig. 1). The molecular mechanisms by which hyperpolymerization of cortical actin attenuated the  $\text{Ca}^{2+}$  buffering or reuptake in these eggs are only a matter of speculation. In view of the fact that ion channels and

pumps on the plasma membrane and the ER are closely associated with the actin cytoskeleton, it is no surprise that the  $\text{Ca}^{2+}$  transport activities are modulated by the state of the local actin cytoskeleton that may alter the positioning or microenvironment of the  $\text{Ca}^{2+}$ -mobilizing channel components [30–34]. By the same token, it is conceivable that hyperpolymerization of cortical actin by PHAL and JAS might have negatively affected the  $\text{Ca}^{2+}$ -reuptake activities of the  $\text{Ca}^{2+}$ -ATPases on the ER or on the plasma membrane and thereby led to an elevated plateau of the residual  $\text{Ca}^{2+}$  level (Fig. 4). Indeed, it has been shown that treatment of hippocampal neurons with JAS synergizes thapsigargin that increases cytosolic  $\text{Ca}^{2+}$  by primarily inhibiting the  $\text{Ca}^{2+}$  uptake through the ER  $\text{Ca}^{2+}$ -ATPase [35]. Alternatively, the elevated plateau at the decaying phase of  $\text{Ca}^{2+}$  response might have happened because the monomeric actin pools in the cytoplasm were depleted due to the hyperpolymerization. Binding of  $\text{Ca}^{2+}$  by G-actin and its incorporation into actin filaments could serve as a supplemental mechanism to absorb  $\text{Ca}^{2+}$  and alleviate its local surge [19,36–39]. Thus, overstabilization of the actin filaments by PHAL and JAS might have repressed the  $\text{Ca}^{2+}$ -removal process by suppressing treadmill. Nonetheless, it bears an emphasis that the functional mechanisms and the effects of the actin drugs are highly intricate, and that it is difficult to explain all our observations solely based on the direction of actin polymerization and depolymerization. Hence, the question of how the actin cytoskeleton affects the biological process of  $\text{Ca}^{2+}$  signaling and sperm entry awaits further investigation in various model systems.

Finally, we found that the time span for the  $\text{Ca}^{2+}$  wave to travel from the sperm interaction site to the antipode was significantly increased not only by CYT-B or LAT-A (see Results), but also by PHAL and JAS. The 'travel time' in the PHAL-treated eggs was  $20.3 \pm 2.9$  s ( $n = 29$ ) as opposed to  $16.8 \pm 2.0$  s of the control eggs ( $n = 25$ ,  $P < 0.0001$ ). Likewise, the travel time in the JAS-pretreated eggs was much longer ( $25.6 \pm 3.3$  s,  $n = 15$ ) than in their control eggs ( $19.8 \pm 2.8$  s,  $n = 22$ ;  $P < 0.0001$ ). Thus, the planar speed of the  $\text{Ca}^{2+}$  wave in the PHAL- and JAS-pretreated eggs at fertilization was also reduced by 17% and 23%, respectively, in comparison with their corresponding control eggs. Taken together, our results in sea urchin eggs again indicated that the actin cytoskeleton plays comprehensive roles at the early stages of egg activation by setting the tone for the excitability of the subplasmalemmal and cytoplasmic matrix and thereby contributes to sperm receptivity at fertilization.

## Acknowledgment

We are grateful to Mr. D. Caramiello and the staffs at the MARER of Stazione Zoologica Napoli (SZN) for the management of the animals, and to Mr. G. Gagnaniello for the assistance in preparing figures. N. Limatola has been financially supported by SZN PhD fellowship.

## References

- [1] R.A. Steinhardt, D. Epel, Activation of sea-urchin eggs by a calcium ionophore, *Proc. Natl. Acad. Sci. U.S.A.* 71 (1974) 1915–1919.
- [2] L.F. Jaffe, Classes and mechanisms of calcium waves, *Cell Calcium* 14 (1993) 736–745.
- [3] J.T. Chun, L. Santella, Intracellular calcium waves, in: W.J. Lennarz, M.D. Lane (Eds.), *The Encyclopedia of Biological Chemistry*, vol. 2, Academic Press, Waltham, MA, USA, 2013, pp. 640–647.
- [4] R. Steinhardt, R. Zucker, G. Schatten, Intracellular calcium release at fertilization in sea urchin egg, *Dev. Biol.* 58 (1977) 185–196.
- [5] T. Schmidt, C. Patton, D. Epel, Is there a role for the  $\text{Ca}^{2+}$  influx during fertilization of the sea urchin egg?, *Dev. Biol.* 90 (1982) 284–290.
- [6] A. McDougall, I. Gillot, M. Whitaker, Thimerosal reveals calcium-induced calcium release in unfertilized sea urchin eggs, *Zygote* 1 (1993) 35–42.
- [7] S.S. Shen, W.R. Buck, Sources of calcium in sea urchin eggs during the fertilization response, *Dev. Biol.* 157 (1993) 157–169.



- [8] L.A. Jaffe, A.F. Giusti, D.J. Carroll, et al.,  $\text{Ca}^{2+}$  signalling during fertilization of echinoderm eggs, *Semin. Cell Dev. Biol.* 12 (2001) 45–51.
- [9] L. Santella, D. Lim, F. Moccia, Calcium and fertilization: the beginning of life, *Trends Biochem. Sci.* 29 (2004) 400–408.
- [10] M. Whitaker, Calcium at fertilization and in early development, *Physiol. Rev.* 86 (2006) 25–88.
- [11] L. Santella, F. Vasilev, J.T. Chun, Fertilization in echinoderms, *Biochem. Biophys. Res. Commun.* 425 (2012) 588–594.
- [12] G.A. Nusco, J.T. Chun, E. Ercolano, et al., Modulation of calcium signaling by the actin-binding protein cofilin, *Biochem. Biophys. Res. Commun.* 348 (2006) 109–114.
- [13] J.T. Chun, F. Vasilev, L. Santella, Antibody against the actin-binding protein depactin attenuates  $\text{Ca}^{2+}$  signaling in starfish eggs, *Biochem. Biophys. Res. Commun.* 441 (2013) 301–307.
- [14] K. Kyoizuka, J.T. Chun, A. Puppo, et al., Guanine nucleotides in the meiotic maturation of starfish oocytes: regulation of the actin cytoskeleton and of  $\text{Ca}^{2+}$  signaling, *PLoS One* 4 (2009) e6296.
- [15] J.T. Chun, A. Puppo, F. Vasilev, et al., The biphasic increase of PIP2 in the fertilized eggs of starfish: new roles in actin polymerization and  $\text{Ca}^{2+}$  signaling, *PLoS One* 5 (2010) e14100.
- [16] K. Kyoizuka, J.T. Chun, A. Puppo, et al., Actin cytoskeleton modulates calcium signaling during maturation of starfish oocytes, *Dev. Biol.* 320 (2008) 426–435.
- [17] A. Puppo, J.T. Chun, G. Gragnaniello, et al., Alteration of the cortical actin cytoskeleton deregulates  $\text{Ca}^{2+}$  signaling, monospermic fertilization, and sperm entry, *PLoS One* 3 (2008) e3588.
- [18] D. Lim, K. Lange, L. Santella, Activation of oocytes by latrunculin A, *FASEB J.* 16 (2002) 1050–1056.
- [19] F. Vasilev, J.T. Chun, G. Gragnaniello, et al., Effects of ionomycin on egg activation and early development in starfish, *PLoS One* 7 (2012) e39231.
- [20] E.E. Just, *The Biology of the Cell Surface*, R. Blakiston's Son & Co., Inc, Philadelphia, USA, 1939, pp. 147–205.
- [21] B. Dale, A. De Santis, The effect of cytochalasin B and D on the fertilization of sea urchins, *Dev. Biol.* 83 (1981) 232–237.
- [22] B. Dale, L.J. De Felice, V. Taglietti, Membrane noise and conductance increase during single spermatozoon-egg interactions, *Nature* 275 (1978) 217–219.
- [23] F.R. Lillie, The mechanism of fertilization, *Science* 38 (1913) 524–528.
- [24] J. Loeb, On some non-specific factors for the entrance of the spermatozoon into the egg, *Science* 40 (1914) 316–348.
- [25] L. Santella L, N. Limatola, J.T. Chun, Actin cytoskeleton and fertilization in starfish eggs, in: H. Sawada (Ed.), *Sexual Reproduction in Animals and Plants*, Springer Verlag, Japan, 2014, pp. 147–155.
- [26] L.A. Jaffe, Fast block to polyspermy in sea urchin eggs is electrically mediated, *Nature* 261 (1976) 68–71.
- [27] B. Dale, Is the idea of a fast block to polyspermy based on artifact?, *Biochem. Biophys. Res. Commun.* 450 (2014) 1159–1165.
- [28] B. Dale, L. DeFelice, Polyspermy prevention: facts and artifacts?, *J. Assist. Reprod. Genet.* 28 (2011) 199–207.
- [29] C.A. Ziomek, D. Epel D, Polyspermy block of *Spisula* eggs is prevented by cytochalasin B, *Science* 189 (1975) 139–141.
- [30] T. Fujimoto, A. Miyawaki, K. Mikoshiba, Inositol 1,4,5-trisphosphate receptor-like protein in plasmalemmal caveolae is linked to actin filaments, *J. Cell Sci.* 108 (1995) 7–15.
- [31] R.L. Patterson, D.B. van Rossum, D.L. Gill, Store-operated  $\text{Ca}^{2+}$  entry: evidence for a secretion-like coupling model, *Cell* 98 (1999) 487–499.
- [32] T. Sugiyama, Y. Matsuda, K. Mikoshiba, Inositol 1,4,5-trisphosphate receptor associated with focal contact cytoskeletal proteins, *FEBS Lett.* 466 (2000) 29–34.
- [33] K. Fukatsu, H. Bannai, S. Zhang, et al., Lateral diffusion of inositol 1,4,5-trisphosphate receptor type 1 is regulated by actin filaments and 4.1N in neuronal dendrites, *J. Biol. Chem.* 279 (2004) 48976–48982.
- [34] T. Smani, N. Dionisio, J.J. López, et al., Cytoskeletal and scaffolding proteins as structural and functional determinants of TRP channels, *Biochim. Biophys. Acta* 2014 (1838) 658–664.
- [35] Y. Wang, M.P. Mattson, K. Furukawa, Endoplasmic reticulum calcium release is modulated by actin polymerization, *J. Neurochem.* 82 (2002) 945–952.
- [36] K. Lange, Microvillar  $\text{Ca}^{++}$  signaling: a new view of an old problem, *J. Cell Physiol.* 180 (1999) 19–34.
- [37] K. Lange, J. Gartzke, F-actin-based Ca signaling – a critical comparison with the current concept of Ca signaling, *J. Cell Physiol.* 209 (2006) 270–287.
- [38] J.T. Chun, L. Santella, Roles of the actin-binding proteins in intracellular  $\text{Ca}^{2+}$  signalling, *Acta Physiol. (Oxf)* 195 (2009) 61–70.
- [39] L. Santella, J.T. Chun, Actin, more than just a housekeeping protein at the scene of fertilization, *Sci. China Life Sci.* 54 (2011) 733–743.